Available online at www.sciencedirect.com
ScienceDirect
Geochimica et Cosmochimica Acta 72 (2008) 1269–1280
Geochimica et Cosmochimica Acta
www.elsevier.com/locate/gca

Acid–base properties of cyanobacterial surfaces. II: Silica as a chemical stressor influencing cell surface reactivity

S.V. Lalonde [a,*], D.S. Smith [b], G.W. Owttrim [c], K.O. Konhauser [a]

[a] Department of Earth and Atmospheric Sciences, 3-13 Earth Science Building, University of Alberta, Edmonton, Alta., Canada T6G 2E3
[b] Department of Chemistry, Wilfrid Laurier University, Waterloo, Ont., Canada N2L 3C5
[c] Department of Biological Sciences, University of Alberta, Edmonton, Alta., Canada T6G 2E9

Received 20 April 2007; accepted in revised form 1 October 2007

Abstract

Bacteria grow in complex solutions where the adsorption of aqueous species and nucleation of mineral phases on the cell surface may interfere with membrane-dependent homeostatic functions. While previous investigations have provided evidence that bacteria may alter their surface chemical properties in response to environmental stimuli, to our knowledge no effort has been made to evaluate surface compositional changes resulting from non-nutritional chemical stresses within a quantitative framework applicable to surface complexation modeling. We consider here the influence of exposure to silica on cyanobacterial surface chemistry, particularly in light of the propensity for cyanobacteria to become silicified in geothermal environments. Using data modeled from over 50 potentiometric titrations of the unsheathed cyanobacterium *Anabaena* sp. strain PCC 7120, we find that both abiotic geochemical and biotic biochemical-assimilatory factors have important and different effects on cell surface chemistry. Changes in functional group distribution that resulted from growth by different nitrogen assimilation pathways were greatest in the absence of dissolved silica and less important in its presence. Furthermore, out of the three nitrogen assimilation pathways investigated, in terms of surface functional group distribution, nitrate-reducing cultures were least sensitive, and ammonium-assimilating cultures were most sensitive, to changes in media silica concentration. When functional group distributions were plotted as a function of silica concentration, it appears that, with higher silica concentrations, basic groups ($pK_a > 7$) increase in concentration relative to acidic groups ($pK_a < 7$), and the total ligand densities (on a per-weight basis) decreased. The results imply a decrease in both the magnitude and density of surface charge as the net result of growth at high silica concentrations. Thus, *Anabaena* sp. appears to actively respond to growth in silicifying solutions by altering its surface properties in a manner that is likely to be manifested in nature by facilitated surface attachment. We conclude that potentiometric titrations reveal a Gram-negative bacterial surface whose properties are dynamic with respect to both nutrient and geochemical stressors.
Crown copyright © 2007 Published by Elsevier Ltd. All rights reserved.

1. INTRODUCTION

As bacteria generally lack internal membrane-bound structures, they must rely on processes localized to surface membranes for a variety of homeostatic functions including metabolism, nutrient transport, signal transduction, motility, and cell division (Madigan et al., 1997). At the same time, their surface layers serve as the primary interface between bacterium and its extracellular milieu, playing a central role in a cell's ability to survive in the face of chemical and physical stressors.

Furthermore, the surfaces of bacteria are chemically reactive. They are studded with organic chemical functional groups that serve as ligands for the sorption of metals (e.g., Beveridge and Murray, 1980; Beveridge et al., 1982; Daughney and Fein, 1998; Daughney et al., 1998), in turn affecting mineral precipitation and dissolution reactions (Konhauser et al., 1993; Fortin et al., 1997; Warren and Ferris, 1998),

* Corresponding author.
E-mail address: stefan.lalonde@ualberta.ca (S.V. Lalonde).

0016-7037/$ - see front matter Crown copyright © 2007 Published by Elsevier Ltd. All rights reserved.
doi:10.1016/j.gca.2007.10.032

solute transport (e.g., McCarthy and Zachara, 1989; Lindgvist and Enfield, 1992; Corapcioglu and Kim, 1995), and redox reactions (for review, see Konhauser, 2006).

In complex solutions under laboratory conditions, the sorptive behavior of the bacterial surface has been successfully described using surface complexation models (e.g., Fowle and Fein, 1999). Such models have been employed to describe the bacterial surface in thermodynamic terms that are independent of experimental conditions. This enables quantitative predictions for elemental partitioning between the aqueous phase and the bacterial surface. For such models to be useful, potentiometric titrations are required to derive concentration and stability parameters for discrete proton-exchanging organic chemical functional groups (referred heretofore as "ligands") located on the bacterial surface. However, it has become apparent that titration data alone cannot provide mechanistic details of adsorption reactions at a molecular level, as different sets of ligands, modeled using different assumptions regarding how sites are affected by surface electric field effects, may provide equally good fit to potentiometric titration data (Fein et al., 2005). Despite these uncertainties, potentiometric titration remains the most practical method for enumerating the concentration of ligands that may contribute to surface charge and solute adsorption over a wide (3–11) pH range.

Ligand variability between bacterial species, or even inherent to a single species, should be accounted for in modeling approaches, yet the extent to which a bacterium is capable of modifying its outer surface in terms of acid–base behavior is poorly understood. To date, ligand variability inherent to a single bacterial species has been quantitatively evaluated as a function of growth phase (Daughney et al., 2001; Haas, 2004; Lalonde et al., 2008), nutrient availability (Borrok et al., 2004; Haas, 2004), and metabolic pathway (Borrok et al., 2004; Haas, 2004; Lalonde et al., 2008). These factors are of special consideration because they pertain to culturing and cell harvesting procedures that are inherent to the laboratory study of bacterial surfaces, and their influence must be accounted for. However there exist numerous other biologically relevant factors, including a wide variety of geochemical stressors, which are not typically encountered in a laboratory setting, yet may influence cell surface composition. It is the aim of this study to evaluate whether or not chemical stress, in this case growth in media at various degrees of saturation with respect to amorphous silica, may influence the acid–base properties of the cell surface as determined by potentiometric titration.

Silica was chosen as a potential stressor because numerous cyanobacteria have been observed to grow in geothermal environments where the rapid precipitation of amorphous silica results in their complete encrustation (see Konhauser et al., 2004, for review). Laboratory strains have been successfully grown in media with concentrations upwards of 300 ppm Si, where exponential phase growth proceeded concurrently with rapid silica polymerization and precipitation (e.g., Phoenix et al., 2000). In this study, we used potentiometric titration to examine the influence of various silica concentrations on the acid–base properties of the cyanobacterium *Anabaena* sp. strain PCC 7120. Titration data is modeled for discrete ligand concentrations and apparent pK_a constants in a non-electrostatic approach, and the results are statistically evaluated for confidence between condition parameters in a pairwise fashion. A discrete ligand model was chosen over a continuous affinity approach for facility of statistical comparison, as well as applicability of discrete ligand data to surface complexation modeling efforts. Conditions of 300 ppm NaCl and 300 ppm Si as powdered silica are also evaluated as potential chemical stressors. As ligand variability for this organism has been reported to arise as a function of nitrogen assimilation pathway (Lalonde et al., 2008), we also conducted our experiments using different nitrogen sources for cell growth. Finally, we evaluate the combined effects of silica concentration and nitrogen fixation pathway as determinants of cell surface reactivity.

2. METHODS

2.1. Growth procedures

The cyanobacterial strain used in this study, *Anabaena* sp. strain PCC 7120, was chosen for its capacity for nitrogen fixation, high rate of growth, and lack of sheath or S-layer (Rippka et al., 1979). The methodology of Lalonde et al. (2008) was applied for all growth, preparation, titration, and modeling procedures.

Cultures limited to growth by ammonium assimilation, assimilatory nitrate reduction, and nitrogen fixation were separately maintained in 50 ml of nitrogen-free liquid BG-11(0) media buffered to pH 8 with 10 mM Tricine and supplemented with 17.6 mM ammonium as NH_4Cl, 17.6 mM nitrate as $NaNO_3$, or 17.6 mM NaCl (no fixed nitrogen source) wherever required. BG-11 ingredients containing fixed nitrogen (ferric ammonium citrate and cobaltous nitrate hexahydrate) were replaced with nitrogen-free equivalents (ferric citrate and cobaltous chloride hexahydrate). As per Chamot and Owttrim (2000), cultures were grown at 30 °C under a constant illumination of ~100 microeinsteins/m^2/s, bubbled with humidified air, and orbitally shaken (50 ml cultures) or magnetically stirred (1-L cultures) at 150 rpm. Cultures limited to a single nitrogen source over at least three transfers were prepared as a source of inoculum (10% v/v) for larger 1-L cultures representing each nitrogen source and prepared to contain mineralizing and control compounds. For all three nitrogen sources, 1 L silica-treated cultures were prepared by the addition of sodium metasilicate to concentrations of 55 and 300 ppm Si. For nitrate-reducing growth only, conditions of 300 ppm NaCl and 300 ppm Si as powdered silica (powdered silicic acid, Fisher Scientific) were also prepared. Powdered silica or the appropriate salt was added prior to autoclaving, and media containing silica were adjusted to pH 8 with KOH immediately prior to inoculation. In the case of 300 ppm sodium metasilicate conditions, neutralization induced a state of supersaturation such that amorphous silica precipitated spontaneously, with monomeric silica concentrations approaching 70 ppm Si after 36 h. Cultures with 55 ppm Si were just below saturation with respect to amorphous silica, and remained stable in monomeric silica concentration

over time. Media containing powdered silica was allowed to equilibrate for 3 days after neutralization and prior to inoculation, and contained stable clay-sized silica particles throughout the experimental duration. All cultures were harvested at stationary phase growth, indicated by an absorbance of 0.6 ± 0.03 (~0.24 g dry bacteria/L), in order to better approximate natural conditions.

All biomass was washed immediately upon harvesting, stored at room temperature and titrated within 18 h of harvesting. Cells centrifuged from each liter of culture were washed three times with 200 ml of 18 MΩ water, four times with 0.01 M KNO_3 titration electrolyte, and resuspended in 0.01 M KNO_3 to a final volume of 50 ml. For each condition, the final 50 ml of concentrated (~4 g dry bacteria/L) biomass was divided to provide five replicate titrations.

2.2. Potentiometric titrations

Solutions were prepared using standard analytical methods (Harris, 1995) and glassware was prewashed according the methodology of Cox et al. (1999). A 0.01-M titration electrolyte was prepared using KNO_3 salt, while 0.01 M NaOH and 0.2 M HNO_3 solutions were prepared from concentrate and standardized by titration against dried KHP prior to use. All solutions were prepared using water purged of dissolved CO_2 with N_2(g) for at least 30 min and maintained under a nitrogen atmosphere.

Titration suspensions were prepared by weight with the addition of ~10 g of concentrated, electrolyte-washed biomass suspension to ~40 g of electrolyte solution in a titration flask under a constant purge of N_2 gas. A Ross-type glass pH electrode (Man-Tech Associates Inc., Guelph, Ontario) was calibrated using commercial buffers and installed in the flask along with a thermocouple, magnetic stir bar, bubbler, and titrant dispenser. No junction potential corrections were applied, although the ionic strength of the buffer solutions (0.05) and titration electrolyte (0.01) were similar. After acidification of the titration suspension to pH ~ 3.2 with 200 µl 0.2 M HNO_3, and upon 30 min of equilibration, titrations were performed alkalimetrically from pH ~ 3.2 to 11 using a QC-Titrate autotitrator (Man-Tech Associates Inc., Guelph, Ontario) delivering CO_2-free 0.01 M NaOH. pH resolution was set to 0.1 and electrode stability criteria to <1 mV/s for each step. Titration from pH ~3.2 to 11 took approximately 50 min on average. After titration, the bacterial suspensions were filtered onto preweighed Whatman GF/C #42 filters (Whatman Inc, Florham park, New Jersey) and oven dried at 70 °C for 48 h prior to weighing. It should be noted that dry bacterial mass units are employed throughout the manuscript, as opposed to wet mass; an average bacterial dry-to-weight mass ratio of 1:8 (Borrok et al., 2005) may serve as a guideline for comparison to other reported values. All conditions were represented by five replicate titrations, and in each case cellular integrity was confirmed by pigment autofluorescence using a Zeiss Axioskop 2 epi-fluorescent light microscope. Titration data presented by Lalonde et al. (2008) for stationary phase *Anabaena* cultures was obtained using identical protocols and is used here to represent silica-free controls.

2.3. Modeling of surface ligand concentrations

Discrete bacterial surface site concentrations were fit to the titration data using a non-electrostatic linear-programming pK_a spectrum approach described in detail by Lalonde et al. (2008) and previously applied to a variety of potentiometric titration studies (Brassard et al., 1990; Cox et al., 1999; Smith and Kramer, 1999; Smith et al., 1999; Martinez and Ferris, 2001; Martinez et al., 2002; Phoenix et al., 2002; Fein et al., 2005). It was determined by replicate blank titration that experimental error had a negligible effect on system charge balance between pH ~3.5 and ~10.3, and data was selected in the 4–10 pH range for the modeling of ligand concentrations over a pK_a range of 3–11 in 0.2 increments. Excess in the charge balance of the system is assumed to result solely by the speciation of proton-exchanging ligands on the bacterial surface, as represented by the following charge balance:

$$\sum_{j=1}^{n}[L_j^-] - [ANC] = C_{bi} - C_{ai} + [H^+]_i - [OH^-]_i \quad (1)$$

where, for the *i*th addition of titrant, Cb and Ca are the concentrations of base and acid, respectively, $[H^+]$ and $[OH^-]$ are measured by the pH electrode, $[L_j^-]$ is the concentration of deprotonated functional groups for the *j*th monoprotic site of *n* possible sites set by the pK_a spectrum, and the acid neutralizing capacity (ANC) functions as a constant offset in charge excess. The bacterial ligand concentrations and ANC that provide the best fit to the measured charge excess (right hand side of Eq. (1)) is determined iteratively by minimizing the absolute error between measured and fitted charge excess (left hand side of Eq. (1)). The number of distinct pK_a sites that are required to describe the data is minimized as the linear-programming approach allows a concentration of zero as a possible solution, and pK_a values were not corrected for surface electrostatic potential in order to avoid assumptions regarding uniformity in cell surface area and specific capacitance. All replicate titrations were modeled independently in order to provide estimates of variance for statistical purposes. The non-electrostatic model employed herein, along with its assumptions, sources of error, and relevance to other bacterial surface charge modeling approaches, is discussed in greater detail in Lalonde et al. (2008).

3. RESULTS AND DISCUSSION

3.1. Charge excess

Measured charge excess (data points, derived acid–base data from the right hand side of Eq. (1)) and fitted charge excess (line obtained by model optimization of the left hand side of Eq. (1)) representing sodium metasilicate conditions and silica-free controls are plotted as a function of nitrogen source and silica concentration in Fig. 1. Rapid changes in charge excess, corresponding to increased surface buffering capacity, occurred at pH extremes for all conditions tested and have been previously reported for titrations of Gram-negative bacterial surfaces (Haas et al., 2001, 2004; Lalonde et al., 2008). Ligands with dissociation constants that lie

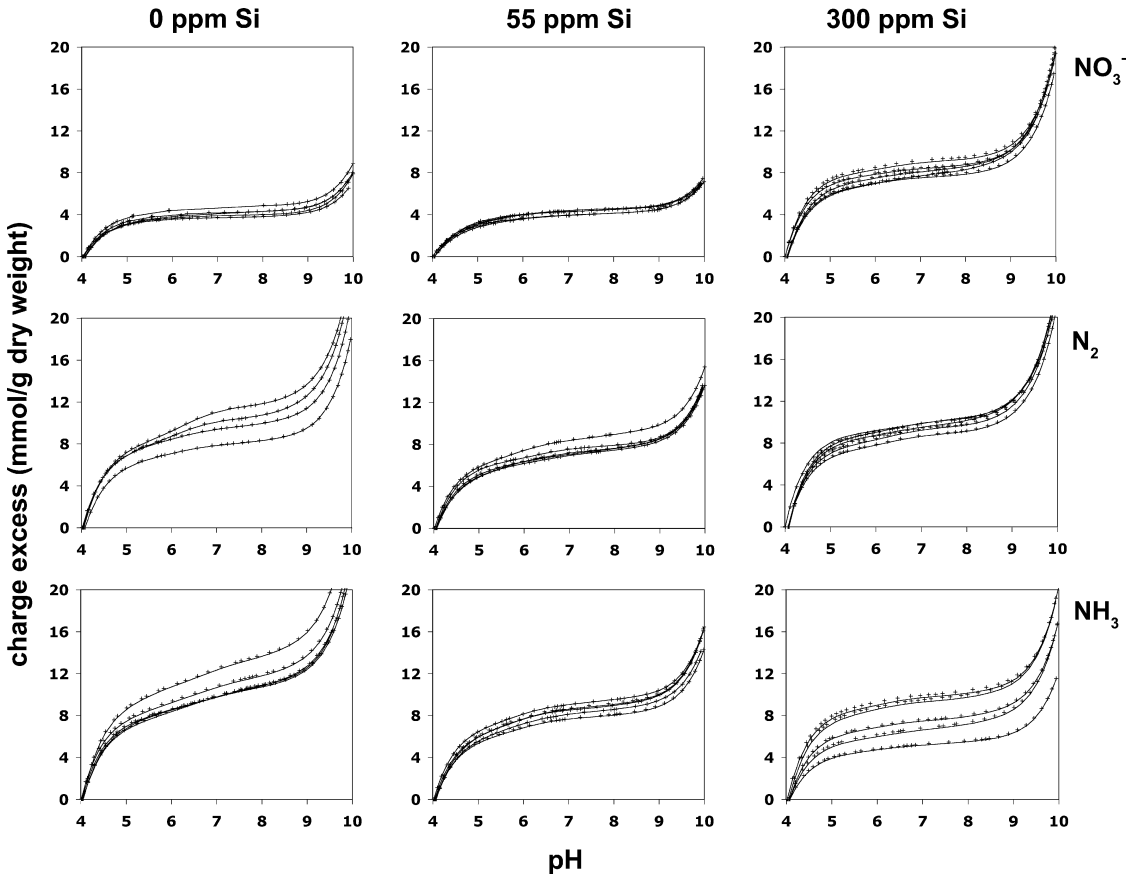

Fig. 1. *Anabaena* surface charge excess arising during alkalimetric titration, plotted as a function of media nitrogen source and silica concentration. Silica was provided as sodium metasilicate, and conditions of 55 ppm Si were approximately saturated with respect to amorphous silica. Conditions of 300 ppm Si were rendered supersaturated with respect to amorphous silica such that the rapid polymerization of silica occurred during growth. For each condition, data points represent charge excess data from five replicate titrations, and smooth curves represent charge excess as fit by discrete ligand modeling.

outside of the pH 4–10 range, such as some acidic carboxyl and basic hydroxyl functional groups, may be responsible for buffering in this region, although increasing uncertainty in measured charge excess at extreme pH (Smith et al., 1999), and a lack of charge excess inflection within the titration range, prevents their accurate quantification. Modeling was performed over a pK_a range of 3–11 to allow for the consideration of ligands with pK_a values outside the 4–10 range, in order to provide a better fit to the charge excess data spanning the pH 4–10 range (see Lalonde et al., 2008, for more detailed discussion). The charge excess curves are presented in Fig. 1 for the qualitative assessment of replicate repeatability and the evaluation of condition-specific charging profiles.

3.2. Modeled parameters

Modeled parameters for all conditions are presented in Table 1, and sodium metasilicate conditions are summarized by pK_a distribution plots in Fig. 2. As evident in Fig. 2, ligand distributions varied sufficiently between conditions as to preclude the assignment of specific sites that are conserved between all conditions. For this reason, mean ligand concentrations are grouped by acidic (ligands with pK_a values between 4 and 7) and basic (ligands with pK_a values between 7 and 10) categories in Table 1, enabling pairwise comparison and statistical correlation between conditions (discussed below).

Ligand pK_a distribution plots (Fig. 2) present, for each condition, ligand concentrations compounded at each possible pK_a value over all five replicates and weighted by the sum dry weight of all five replicates. All conditions return non-zero concentrations for both acidic and basic ligand categories, and variability is evident between all conditions in ligand concentration, pK_a distribution, and the number of distinct sites invoked by the pK_a spectrum model.

Several general, qualitative observations can be made regarding the composite plots shown in Fig. 2. For conditions with 300 ppm Si, ligands with pK_a values below ~6 are noticeably absent and the concentration of basic ligands increases relative to conditions with 55 or 0 ppm Si. It is unlikely that these basic ligands represent the ionization of silicic acid that were retained through the washing procedure; although soluble silicic acid has a pK_a of 9.8 (Iler, 1979), surface sites on colloidal and particulate silica have ionization constants of ~7.5 (Kobayashi et al., 2005), and such sites are absent in the composite plots for 300 ppm Si even though the colloidal silica is more likely to have been trans-

Table 1
Modeled ligand concentrations (in mmol per dry g) and pK_a distributions for all conditions tested

pK_a	4–7	7–10	Ratio (acidic to basic)	Total
NO_3 0 ppm Si	1.24 ± 0.08	0.30 ± 0.05	4.11	1.55 ± 0.10
NO_3 55 ppm Si	1.58 ± 0.19	0.20 ± 0.05	7.74	1.79 ± 0.20
NO_3 300 ppm Si	1.10 ± 0.08	0.99 ± 0.13	1.10	2.09 ± 0.15
NO_3 300 pm NaCl	2.13 ± 0.15	0.42 ± 0.06	5.05	2.55 ± 0.15
NO_3 300 ppm Si[a]	4.00 ± 0.39	8.26 ± 0.69	0.48	12.25 ± 0.54
N_2 0 ppm Si	2.85 ± 0.49	0.18 ± 0.18	16.19	3.02 ± 0.65
N_2 55 ppm Si	1.93 ± 0.09	0.57 ± 0.11	3.40	2.50 ± 0.18
N_2 300 ppm Si	1.39 ± 0.07	1.97 ± 0.22	0.71	3.36 ± 0.18
NH_4 0 ppm Si	2.18 ± 0.23	1.70 ± 0.10	1.28	3.88 ± 0.31
NH_4 55 ppm Si	2.29 ± 0.12	0.55 ± 0.03	4.14	2.85 ± 0.11
NH_4 300 ppm Si	1.12 ± 0.08	0.69 ± 0.10	1.63	1.81 ± 0.14
Average[b]	1.79 ± 0.10	0.71 ± 0.10	2.54	2.50 ± 0.15

Si concentrations describe cultures supplemented with sodium metasilicate unless otherwise noted. Values are the average of five independently modeled titrations. Uncertainties are one standard error of the mean.
[a] Si as particulate silica.
[b] Average values reported here exclude 300 ppm NaCl and colloidal silica conditions.

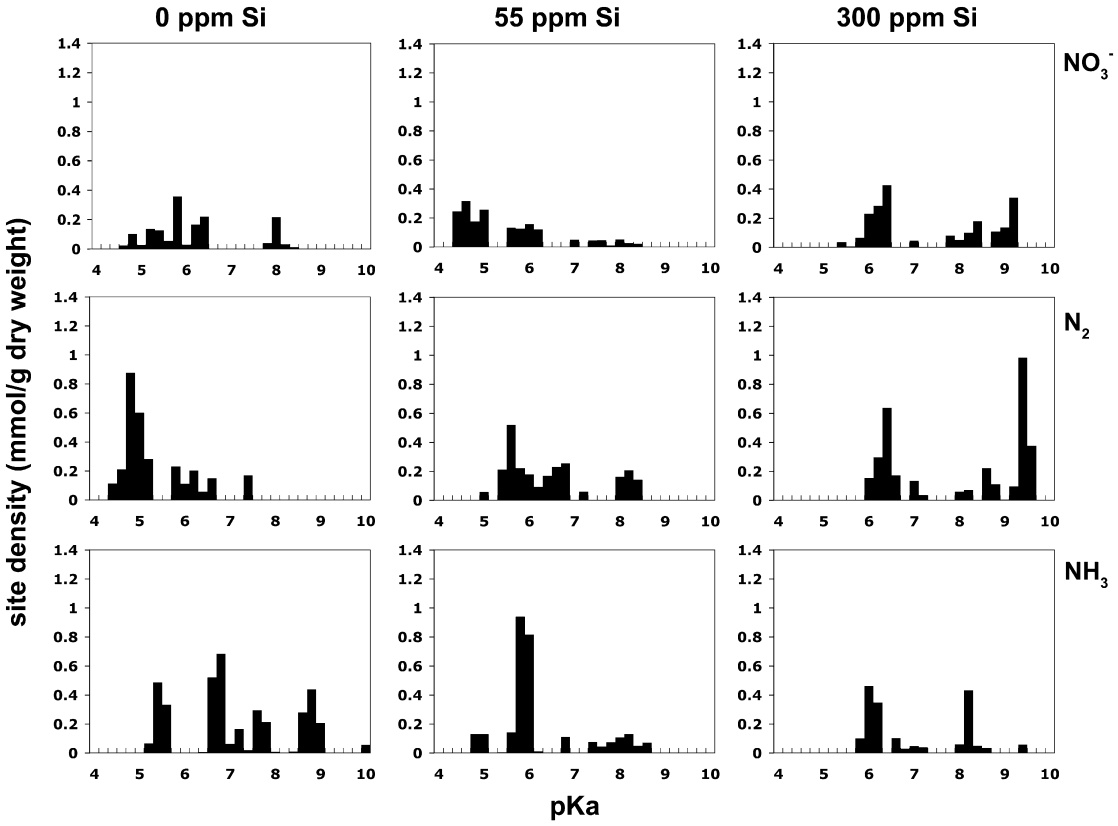

Fig. 2. Modeled ligand distributions grouped as a function of media nitrogen source and silica concentration. Silica conditions correspond to those described for Fig. 1. Each plot accounts for five replicate alkalimetric titrations, with ligand concentrations weighted by occurrence at each pK_a interval.

ferred along with cells during washing than the soluble silicic acid.

Conditions with 0 and 55 ppm Si generally indicate cell surfaces dominated by acidic ligands, in concurrence with the overall negative surface charge typically displayed by both Gram-negative and Gram-positive bacteria (Bayer and Sloyer, 1990). Electrophoretic assessment of surface charge was attempted over the course of this study, however, the filamentous nature of *Anabaena* introduced chain-length effects and other random errors that prevented any conclusions beyond a neutral to negatively charged surface for all conditions assessed (data not shown).

Based on previous spectroscopic investigations (Yee et al., 2004; Jiang et al., 2004), ligands with pK_a values between 8 and 10 likely represent amine functional groups contributing positive charge at neutral pH, as phenolic hydroxyl functional groups display dissociation constants between 9.9 and 10.8 (Martell and Smith, 1977) and at least for Gram-positive bacteria, have not been considered important constituents of major cell wall components (Cox et al., 1999). Within the Gram-negative cell wall, peptidoglycan, proteins, and lipoproteins all possess amine functional groups, sometimes at more than one location per polymer unit, and spectroscopic methods confirm their abundance on the bacterial surface (Yee et al., 2004; Jiang et al., 2004). As protonated amine functional groups are the only proton-exchanging ligands conferring positive charge to the bacterial surface, it follows that the direction and degree of electrical charge on a bacterial surface free of sorbed contaminants is primarily determined at any pH by the balance in concentration between protonated amine functional groups and deprotonated acidic functional groups conferring negative charge. Variability in ligand distribution between conditions is discussed in this context after statistical treatments outlined below.

3.3. Sodium chloride and particulate silica stress

Conditions of 300 ppm NaCl and 300 ppm Si as particulate silica were also investigated for nitrate-reducing cultures, and the results are included in Table 1 and summarized graphically in Fig. 3. These conditions were performed on nitrate-reducers out of consideration for the large body of genetic knowledge regarding the cyanobacterial salt stress response (discussed below).

For nitrate-reducing conditions of 300 ppm NaCl, the ligand pK_a distribution is dominated by a single ligand with p$K_a \sim 7$, in contrast to those representing nitrate-reducing cultures grown in the presence or absence of silica. This may be, in part, reconciled by previous efforts that have revealed numerous expressional changes in both membrane and cytoplasmic proteins that are induced by osmotic and salt stress. For the halotolerant cyanobacterium *Anabaena torulosa*, as many as 90 genes are induced in response to salt-stress (Apte and Bhagwat, 1989; Apte and Haselkorn, 1990), and for *Synechocystis* sp. strain PCC 6803, about 240 genes are upregulated 3-fold within the first 30 min of exposure to salt, decreasing to 39 after 24 h (Marin et al., 2004). Detailed study has demonstrated that overexpression of a Na^+/H^+ antiporter confers salt tolerance to *Synechococcus* sp. strain PCC 7942 (Waditee et al., 2002). While the influence of changes in membrane protein expression on bulk acid–base microbial surface characteristics remains unknown, the increased importance of transmembrane structures whose function or conformation is dependent on pH, as is the case with the Na^+/H^+ transporter (Putney et al., 2002), could account for the differences observed as the result of growth in media with 300 ppm NaCl. Interestingly, salt-stress-induced proteins previously identified from two different strains of *Anabaena* have isoelectric points between 5.8 and 7.5 (Apte and Bhagwat, 1989).

Results obtained from conditions of 300 ppm Si (as particulate silica) are also presented in Fig. 3, and display the largest deviation from other conditions in both charge excess and ligand distribution. The charge excess curve shows increased buffering over the entire titration range, and the modeled ligand concentrations were in total approximately six times higher than other conditions, with ligands largely

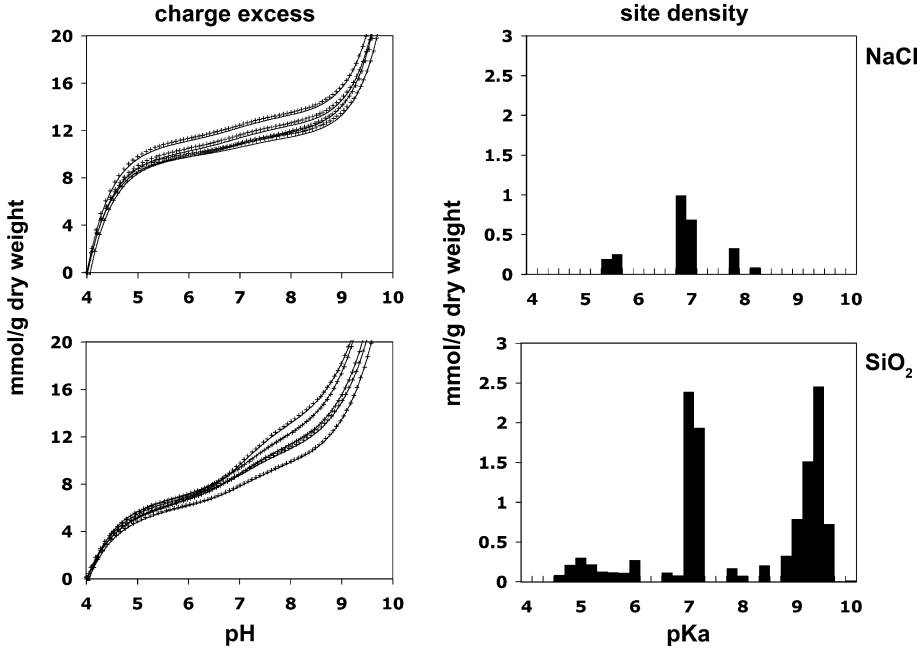

Fig. 3. Plots of charge excess and corresponding modeled ligand distributions for *Anabaena* grown under nitrate-reducing conditions with 300 ppm NaCl and 300 ppm Si as particulate silica. Both measured (data points) and fitted (smooth curves) charge excess is presented for five replicates, and ligand distributions are weighed by occurrence and compounded over five replicates.

distributed between ligands with pK_a 7 and 9. It should be noted that the mode of growth in the presence of particulate silica was different relative to all other conditions; silica particles were rapidly covered by *Anabaena* cells, and the cultures were dominated by clumps of bacteria–silica aggregates, in contrast to the well-dispersed nature of *Anabaena* cells grown under all other conditions. The incomplete separation of bacteria from silica during washing is possibly responsible for the elevated ligand concentrations observed for this condition. An intrinsic ionization constant of 7.5 has been predicted for surface sites of particulate silica on the basis of the multisite surface complexation (MUSIC) model and estimated by potentiometric titration to be 7.6 (Kobayashi et al., 2005), and the first deprotonation of monosilicic acid occurs ~9.8 (Iler, 1979). The titrations of this condition (SiO_2, Fig. 3) indicate that particulate silica was not wholly removed from the bacterial surface prior to titration by the washing procedure employed herein.

3.4. Sources of ligand variability

In order to ascertain the sources of variability between the examined conditions, pairwise indices of confidence in comparisons between ligand concentrations were generated using the Tukey–Kramer test in ANOVA post-hoc analysis. The Tukey–Kramer test, a variant of the Tukey HSD test that employs a harmonic mean to account for unequal sample sizes, allows for a large number of pairwise comparisons to be made while maintaining an overall type I error rate at the desired level of significance (0.05 in this case) (Hsu, 1996). Statistical treatments relying on multiple, independent pairwise comparisons (e.g., using a Student's t test or one-way ANOVA) suffer from a type I error rate that increases with the number of comparisons made. The Tukey–Kramer test accounts for an increasing number of pairwise comparisons by decreasing the confidence in difference between pairs according to the studentized range distribution.

Modeled parameters were broadly classified as acidic (pK_a < 7) or basic (pK_a > 7) in order to simplify the comparison of ligands between conditions and to select for only important changes with respect bulk acid–base surface properties. The average parameters from conditions of 300 ppm Si as particulate silica were considered outliers and excluded from Tukey–Kramer analysis. The mean ligand concentrations being compared are summarized in Table 1. Three distinct rounds of Tukey–Kramer analysis were performed, one for each class of ligand concentration (acidic or basic) and one for total ligand concentration, and each round comprised all pairwise comparisons between 11 mean concentrations (mean concentrations from 10 conditions of $n = 5$, and the mean of those concentrations with $n = 50$). Two-tailed confidence intervals for all pairwise comparisons are presented for reference in Table 2. A confidence interval greater than 0.95 indicates statistically significant similarity in concentration, while a confidence interval less than 0.05 indicates statistically significant difference.

In order to distinguish trends in the similarity of parameters across conditions, two-tailed confidence intervals obtained by Tukey–Kramer analyses are grouped by comparison type in Fig. 4. Pairwise-comparisons between metabolic conditions indicate that differences in ligand distributions resulting from differential metabolism are greatest at 0 ppm Si, less important at 300 ppm Si, and least important at 55 ppm. In other words, metabolic pathway appears to affect ligand distribution most importantly at 0 ppm Si and least importantly at 55 ppm Si. From comparisons between Si concentrations, it is apparent that variability in ligand distribution incurred as the result of silica concentration affected ammonium-assimilating cultures most significantly, while nitrate-reducing cultures were least affected by increasing silica concentration. Interestingly, confidence in comparisons between silica concentrations was often higher for total ligand concentrations than for the concentration of one or both ligand classes, in contrast to metabolic comparisons where confidence in total ligand concentrations was generally accompanied by confidence in individual ligand classes. As a re-distribution of ligands between pK_a classes may not affect total ligand concentration, it would appear that the presence of silica at times induced a redistribution of ligands in pK_a space with lesser affect on total ligand concentration. The above observations are generalizations to which exceptions occur in essentially every case, usually with respect to one or more ligand classes, and should be considered preliminary; it is however clear that the interplay between metabolism and geochemical stressor in determining bacterial surface properties is complex.

3.5. Trends in ligand distribution

Mean ligand concentrations are plotted for all sodium metasilicate conditions as a function of ligand grouping (acidic, basic, total) and Si concentration in Fig. 5. For the purposes of this figure (and in contrast to Tukey–Kramer analysis) conditions of 300 ppm NaCl were omitted along with the conditions of 300 ppm Si as particulate silica. The mean ligand concentrations for each condition were plotted, and a linear regression was applied between Si concentration and the corresponding mean ligand concentration. On average, the concentration of acidic ligands decreased with increasing Si concentration with excellent fit to the linear regression ($R^2 = 0.9997$), while the average concentration of basic ligands generally increased with higher Si concentrations ($R^2 = 0.5221$), although with much greater scatter apparent among data points. A plot of the average concentration ratio of acidic to basic ligands vs. Si concentration highlights their covariance; the average ratio of acidic to basic ligands decreases from over 7:1 to nearly 1:1, with good fit ($R^2 = 0.9693$). One major consequence of such ligand pK_a redistribution is the alteration of effective surface charge; as proton-exchanging ligands are the sole providers of effective surface charge on bacterial surfaces under ideal conditions (Fein et al., 2005), the increased concentration of amine functional groups conferring positive charge at pH values below 8 and decreased contribution of ligands contributing negative charge at pH values below 7 (i.e. carboxyl and phosphoryl) will result in neutralization of the inherent negative charge of the Gram-negative cell wall.

On average, the total ligand concentration also decreased with increasing silica concentration ($R^2 = 0.5967$),

Table 2
Confidence intervals in pairwise comparisons of ligand concentration evaluated by Tukey post-hoc analysis (two-tailed p, $n = 11$, df = 89)

Nitrogen metabolism		NO_3			N_2			NH_4			NO_3
	Geochemical stressor	0 ppm Si	55 ppm Si	300 ppm Si	0 ppm Si	55 ppm Si	300 ppm Si	0 ppm Si	55 ppm Si	300 ppm Si	300 ppm NaCl
Ligands with pK_a from 4 to 7											
NO_3	55 ppm Si	0.98									
	300 ppm Si	1.00	0.80								
N_2	0 ppm Si	0.00	0.00	0.00							
	55 ppm Si	0.33	0.97	0.10	0.05						
	300 ppm Si	1.00	1.00	0.99	0.00	0.69					
NH_4	0 ppm Si	0.04	0.53	0.01	0.36	1.00	0.16				
	55 ppm Si	0.01	0.28	0.00	0.64	0.96	0.06	1.00			
	300 ppm Si	1.00	0.85	1.00	0.00	0.13	1.00	0.01	0.00		
NO_3	300 ppm NaCl	0.06	0.66	0.01	0.26	1.00	0.23	1.00	1.00	0.02	
	Average	0.19	0.99	0.03	0.00	1.00	0.63	0.77	0.40	0.04	0.89
Ligands with pK_a from 7 to 10											
NO_3	55 ppm Si	1.00									
	300 ppm Si	0.00	0.00								
N_2	0 ppm Si	1.00	1.00	0.00							
	55 ppm Si	0.89	0.54	0.30	0.42						
	300 ppm Si	0.00	0.00	0.00	0.00	0.00					
NH_4	0 ppm Si	0.00	0.00	0.00	0.00	0.00	0.89				
	55 ppm Si	0.92	0.60	0.25	0.48	1.00	0.00	0.00			
	300 ppm Si	0.44	0.15	0.77	0.10	1.00	0.00	0.00	1.00		
NO_3	300 ppm NaCl	1.00	0.97	0.04	0.93	1.00	0.00	0.00	1.00	0.88	
	Average	0.09	0.01	0.32	0.00	1.00	0.00	0.00	0.99	1.00	0.56
All ligands											
NO_3	55 ppm Si	1.00									
	300 ppm Si	0.92	1.00								
N_2	0 ppm Si	0.00	0.04	0.28							
	55 ppm Si	0.26	0.68	0.99	0.93						
	300 ppm Si	0.00	0.00	0.03	1.00	0.40					
NH_4	0 ppm Si	0.00	0.00	0.00	0.40	0.01	0.94				
	55 ppm Si	0.02	0.14	0.60	1.00	1.00	0.94	0.16			
	300 ppm Si	1.00	1.00	1.00	0.05	0.72	0.00	0.00	0.16		
NO_3	300 ppm NaCl	0.19	0.58	0.97	0.97	1.00	0.49	0.02	1.00	0.62	
	Average	0.03	0.25	0.92	0.67	1.00	0.06	0.00	0.96	0.30	1.00

and growth of *Anabaena* in supersaturated silica solutions resulted in a cell surface that was on average 20% less reactive over the titration range.

The decrease in the degree and density of negative charge on the cyanobacterial surface has important implications for substrate adherence and colloidal attachment. Microbial adhesion is determined over larger (>1 nm) separation distances by a combination of universally attractive van der Waals forces and generally repulsive electrostatic forces, the latter arising from electrical interactions between negatively charged bacterial cells and natural surfaces which tend to possess negative charges (van Loosdretch et al., 1989). For more hydrophobic surfaces, van der Waals forces will determine bacterial adhesion; however, for more strongly charged hydrophilic cell surfaces, such as the case for planktonic cyanobacteria (Fattom and Shilo, 1984), electrostatic forces become more influential on the adhesion process (van Loosdrecht et al., 1987). Interestingly, Zita and Hermansson (1997) showed a strong correlation between positive charges on the bacterial surface and cell surface hydrophobicity using six different strains of *Escherichia coli*, however their findings remain unconfirmed. The methods utilized in the present study do not allow for conclusions regarding cell surface hydrophobicity, and for the purposes of discussion we assume that hydrophobicity remains unchanged between growth conditions, although this is unlikely the case (van Loosdrecht et al., 1987; Fattom and Shilo, 1984), and that cells of *Anabaena* are likely hydrophilic, as inferred their planktonic habit of growth (Fattom and Shilo, 1984). The net result of decreasing neg-

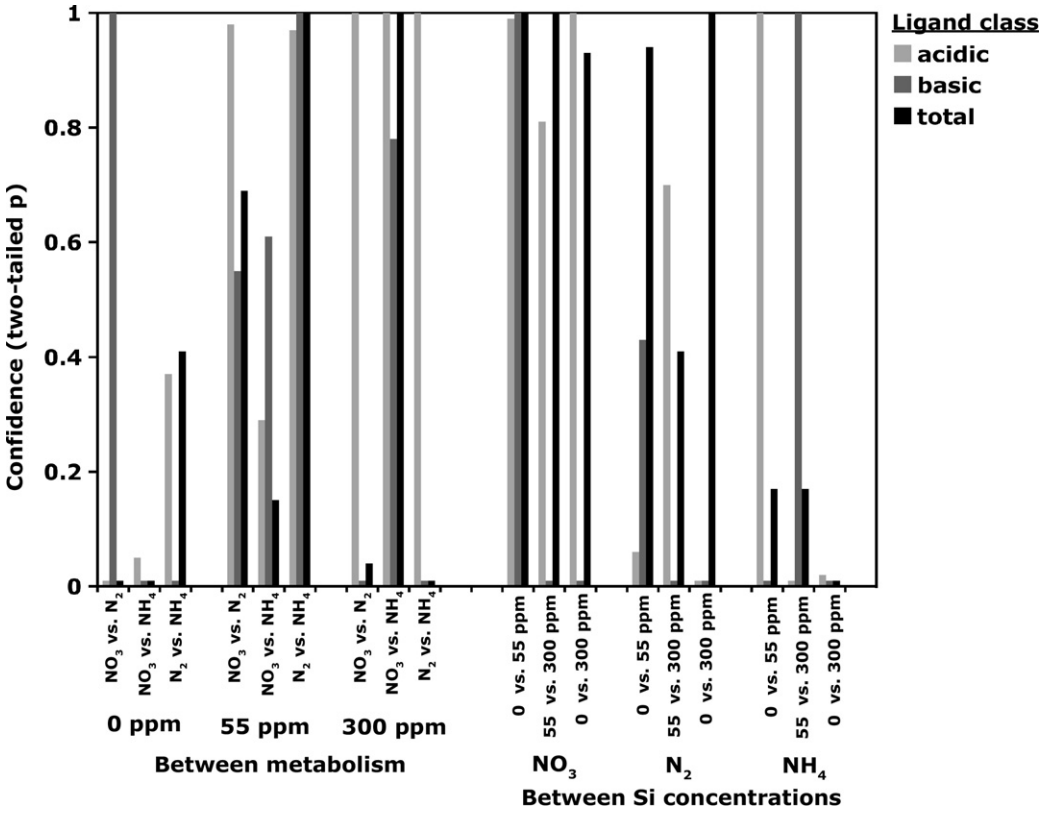

Fig. 4. Confidence intervals in multiple pairwise comparisons of ligand concentration, plotted as a function of comparison type: between-metabolism comparisons grouped as a function of Si concentration (left) and between-Si concentration comparisons grouped as a function of nitrogen metabolism (right).

ative surface charge on the hydrophilic cyanobacterial surface with increasing silica concentration should facilitate attachment to negatively charged surfaces, such as those exposed by particulate and colloidal silica. Walker et al. (2005) similarly indicated that for Gram-negative bacteria, non-specific adhesion is facilitated by changes in cell surface electrical potential and surface charge heterogeneity provided by membrane proteins and lipoproteins.

This trend is not particularly well-suited for the growth of a cyanobacterium in a silicifying solution; decreased electrostatic repulsion between negatively-charged silica species and the negatively-charged bacterial surface will facilitate the adsorption of silica species to the cell surface. As cyanobacteria have been experimentally grown in silicifying solutions at concentrations higher than typically found in natural waters, and have been observed to flourish in silica-depositing geothermal springs (see Konhauser et al., 2004, for review), it is apparent that the adsorption of silica species is not immediately detrimental to many species of cyanobacteria. In fact, the benthic style of growth observed for conditions of 300 ppm Si (as particulate silica) points to an alternative purpose for the modification of ligand distribution; that of surface attachment. As highlighted by van Loosdrecht et al. (1987), benthic and planktonic bacteria modify their surface properties differently in the face of nutrient stress; benthic bacteria become more hydrophilic, promoting surface detachment and recolonization (Malmqvist, 1983; Fattom and Shilo, 1984; Wrangstadh et al., 1986), while starvation promotes surface attachment amongst planktonic bacteria (Dawson et al., 1981; Kjelleberg and Hermansson, 1984). For planktonic bacteria, it is assumed that attachment to suspended solids will increase mobility and favor recolonization (van Loosdrecht et al., 1987). We consider it likely that the results reported here represent a similar survival strategy on the part of *Anabaena*; the cell is capable of modifying the surface concentration of charge-conferring functional groups in response to geochemical stress in order to facilitate potential transport and recolonization. For a planktonic organism such as *Anabaena*, such a response may be poorly suited to survival in hot spring system rapidly precipitating amorphous silica, and it is likely that surface characterization of cyanobacterial strains more typical of hot spring settings, (i.e. mat-forming *Calothrix* and *Phormidium* species) will reveal alternative strategies for survival during silica encrustation (e.g., production or thickening of sheath material, as indicated by Benning et al., 2004). Nonetheless, our results indicate that the cell surface is dynamic, where as a consequence of biological demand a cell may modify its surface properties during growth as a function of stressor concentration. While such changes have been previously indicated using hydrophobicity data (see van Loosdrecht et al., 1987, for summary), we show for the first time that such changes are discernable from potentiometric titration data alone, and in such a way that may be accounted for in a surface complexation modeling approach.

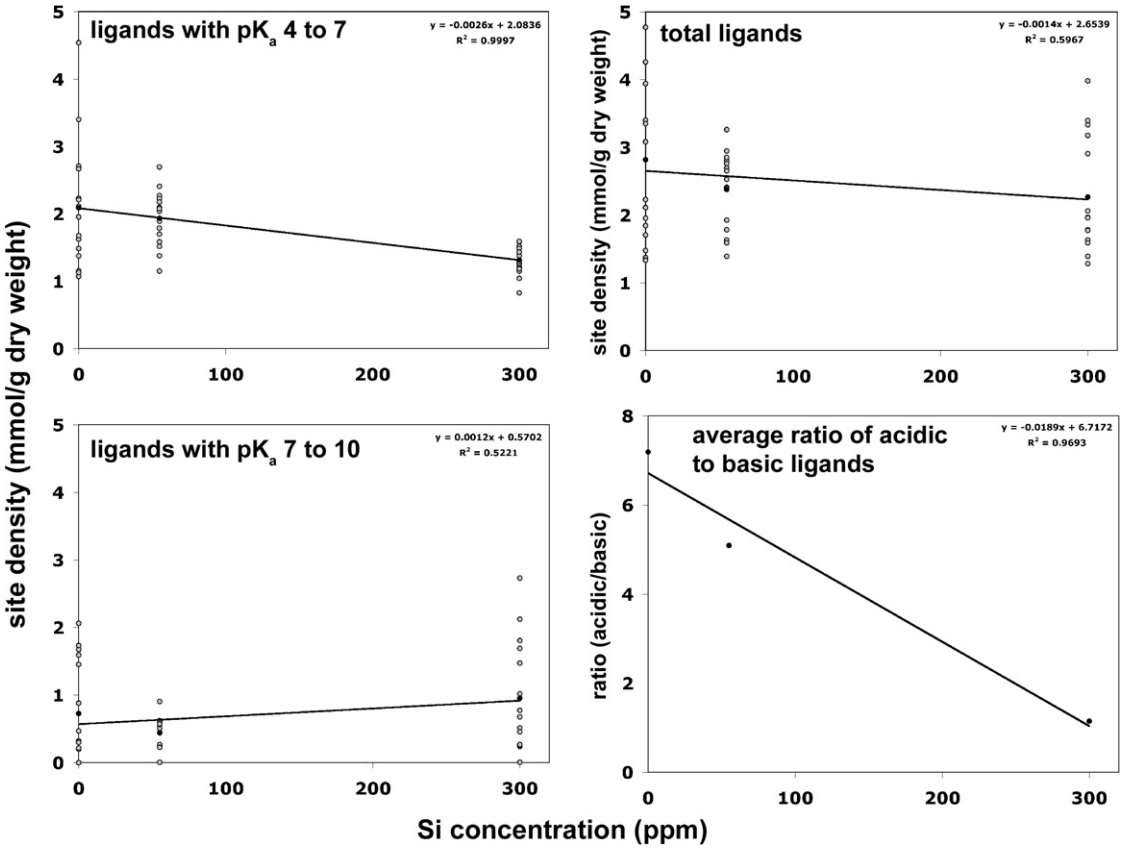

Fig. 5. Average ligand concentrations as a function of ligand class and Si concentration. Also plotted is the average ratio of acidic to basic ligands as function of Si concentration. Grey points represent average ligand concentrations for individual conditions ($n = 5$ at each point) and dark points represent the overall average ligand concentration at that Si concentration ($n = 15$ at each point). Conditions of 300 ppm NaCl and 300 ppm Si as particulate silica are omitted.

4. CONCLUSIONS

The concentration and pK_a distributions of proton-exchanging ligands on the surface of *Anabaena* sp. strain PCC 7120 were modeled from the potentiometric titration of pure cultures and used to investigate the role of silica as a geochemical stressor determining acid–base properties of the bacterial surface. Experiments were performed using stationary phase cells grown under a variety of dissolved silica concentrations and nitrogen assimilation pathways. It was determined that variability in acid–base surface properties attributable to nitrogen metabolism were greatest at 0 ppm Si, and decreased in importance for conditions both undersaturated and supersaturated with respect to amorphous silica. Cultures grown by ammonium assimilation were most sensitive to the presence of silica in terms of acid–base surface properties, while cultures grown by nitrate reduction were the least sensitive to the presence of silica. On average, ligands with pK_a values between 4 and 7 (ligands typically contributing negative charge at circumneutral pH) decreased in concentration with increasing silica concentration, while ligands with pK_a values between 7 and 10 (including amine functional groups contributing positive charge at circumneutral pH) increased with increasing silica concentration. The total site density decreased with increasing silica concentration, and the net effect of exposure to silicifying solutions during growth is proposed to be facilitated non-specific adhesion. These results indicate that a single bacterial species subtly controls surficial acid–base properties in response to geochemical stressors that are independent of nutrition, and that potentiometric titration may be used to quantify such changes within a thermodynamic framework applicable to surface complexation modeling.

REFERENCES

Apte S. K. and Bhagwat A. A. (1989) Salinity-stress-induced proteins in two nitrogen-fixing *Anabaena* strains differentially tolerant to salt. *J. Bacteriol.* **171**, 909–915.

Apte S. K. and Haselkorn R. (1990) Cloning of salinity stress-induced genes from the salt-tolerant nitrogen-fixing cyanobacterium *Anabaena torulosa*. *Plant Mol. Biol.* **15**, 723–733.

Bayer M. E. and Sloyer Jr. J. L. (1990) The electrophoretic mobility of Gram-negative and Gram-positive bacteria: an electrokinetic analysis. *J. Gen. Microbiol.* **136**, 867–874.

Benning L. G., Phoenix V. R., Yee N. and Konhauser K. O. (2004) The dynamics of cyanobacterial silicification: an infrared micro-spectroscopic investigation. *Geochim. Cosmochim. Acta* **68**, 743–757.

Beveridge T. J. and Murray R. G. (1980) Sites of metal deposition in the cell wall of *Bacillus subtilis*. *J. Bacteriol.* **141**, 876–887.

Beveridge T. J., Forsberg C. W. and Doyle R. J. (1982) Major sites of metal binding in *Bacillus licheniformis* walls. *J. Bacteriol.* **150**, 1438–1448.

Borrok D., Fein J. B., Tischler M., O'Loughlin E., Meyer H., Liss M. and Kemner K. M. (2004) The effect of acidic solutions and growth conditions on the adsorptive properties of bacterial surfaces. *Chem. Geol.* **209**, 107–109.

Borrok D., Turner B. F. and Fein J. B. (2005) A universal surface complexation framework for modeling proton binding onto bacterial surfaces in geological settings. *Amer. J. Sci.* **305**, 826–853.

Brassard P., Kramer J. R. and Collins P. V. (1990) Binding site analysis using linear programming. *Environ. Sci. Technol.* **24**, 195–201.

Chamot D. and Owttrim G. W. (2000) Regulation of cold shock-induced RNA helicase gene expression in the cyanobacterium *Anabaena*. sp. strain PCC 7120. *J. Bacteriol.* **182**, 1251–1256.

Corapcioglu M. Y. and Kim S. (1995) Modeling facilitated contaminant transport by mobile bacteria. *Water Resour. Res.* **31**, 2648–2693.

Cox J. S., Smith D. S., Warren L. A. and Ferris F. G. (1999) Characterizing heterogeneous bacterial surface functional groups using discrete affinity spectra for proton binding. *Environ. Sci. Technol.* **33**, 4514–4521.

Daughney C. J. and Fein J. B. (1998) The effect of ionic strength on the adsorption of H^+, Cd^{2+}, Pb^{2+}, and Cu^{2+} by *Bacillus subtilis* and *Bacilllus licheniformis*: a surface complexation model. *J. Colloid Interf. Sci.* **198**, 53–77.

Daughney C. J., Fein J. B. and Yee N. (1998) A comparison of the thermodynamics of metal adsorption onto two common bacteria. *Chem. Geol.* **144**, 161–176.

Daughney C. J., Fowle D. A. and Fortin D. E. (2001) The effect of growth phase on proton and metal adsorption by *Bacillus subtilis*. *Geochim. Cosmochim. Acta* **65**, 1025–1035.

Dawson M. P., Humphrey B. A. and Marshall K. C. (1981) Adhesion: a tactic in the survival strategy of marine *Vibrio* during starvation. *Curr. Microbiol.* **6**, 195–199.

Fattom A. and Shilo M. (1984) Hydrophobicity as an adhesion mechanism of benthic cyanobacteria. *Appl. Environ. Microbiol.* **47**, 135–143.

Fein J. B., Boily J.-F., Yee N., Gorman-Lewis D. and Turner B. F. (2005) Potentiometric titrations of *Bacillus subtilis* cells to low pH and a comparison of modeling approaches. *Geochim. Cosmochim. Acta* **69**, 1123–1132.

Fortin D., Ferris F. G. and Beveridge T. J. (1997) Surface-mediated mineral development by bacteria. In *Geomicrobiology: Interactions Between Microbes and Minerals*, vol. 35 (eds. J. F. Banfield and K. H. Nealson), pp. 161–180. Reviews in Mineralogy and Geochemistry. Mineralogical Society of America, Washington, DC.

Fowle D. A. and Fein J. B. (1999) Competitive adsorption of metal cations onto two Gram-positive bacteria: testing the chemical equilibrium model. *Geochim. Cosmochim. Acta* **63**, 3059–3067.

Haas J. R. (2004) Effects of cultivation conditions on acid–base titration properties of *Shewanella putrefaciens*. *Chem. Geol.* **209**, 67–81.

Haas J. R., Dichristina T. J. and Wade, Jr., R. (2001) Thermodynamics of U(VI) sorption onto *Shewanella putrefaciens*. *Chem. Geol.* **180**, 33–54.

Harris D. C. (1995) *Quantitative Chemical Analysis*. Freeman, New York, NY.

Hsu J. C. (1996) *Multiple Comparisons. Theory and Methods*. Chapman and Hall, London, England.

Iler R. K. (1979) *The Chemistry of Silica: Solubility, Polymerization, Colloidal and Surface Properties, and Biochemistry of Silica*. John Wiley and Sons, New York, NY.

Jiang W., Saxena A., Song B., Ward B. B., Beveridge T. J. and Myneni S. C. B. (2004) Elucidation of functional groups on Gram-positive and Gram-negative bacterial surfaces using infrared spectroscopy. *Langmuir* **20**, 11433–11442.

Kjelleberg S. and Hermansson M. (1984) Starvation-induced effects on bacterial surface characteristics. *Appl. Environ. Microbiol.* **48**, 497–503.

Kobayashi M., Juillerat F., Galletto P., Bowen P. and Borkovec M. (2005) Aggregation and charging of colloidal silica particles: effect of particle size. *Langmuir* **21**, 5761–5769.

Konhauser K. O. (2006) *Introduction to Geomicrobiology*. Blackwell Scientific Publications, Oxford, England.

Konhauser K. O., Fyfe W. S., Ferris F. G. and Beveridge T. J. (1993) Metal sorption and precipitation by bacteria in two Amazonian river systems: Rio Solimoes and Rio Negro. *Brazil. Geol.* **21**, 1103–1106.

Konhauser K. O., Jones B., Phoenix V. R., Ferris G. and Renaut R. W. (2004) The microbial role in hot spring silicification. *Ambio* **33**, 552–558.

Lalonde S. V., Smith D. S., Owttrim G. W. and Konhauser K. O. (2008) Acid–base properties of cyanobacterial surfaces I: influences of growth phase and nitrogen metabolism on cell surface reactivity. *Geochim. Cosmochim. Acta* **72**, 1257–1268.

Lindgvist R. and Enfield C. G. (1992) Cell density and non-equilibrium sorption effects on bacterial dispersal in ground water microcosms. *Microbial Ecol.* **24**, 25–41.

Madigan M. T., Martinko J. M. and Parker J. (1997) *Brock Biology of Microorganisms*, eighth ed. Prentice Hall, Upper Saddle River, NJ.

Malmqvist T. (1983) Bacterial hydrophobicity measured as partition of palmitic acid between the two immiscible phases of cell surface and buffer. *Scand. Sect. B* **91**, 69–73.

Marin K., Kanesaki Y., Los D. A., Murata N., Suzuki I. and Hagemann M. (2004) Gene expression profiling reflects physiological processes in salt acclimation of *Synechocystis* sp. strain PCC 6803. *Plant Physiol.* **136**, 3290–3300.

Martell A. E. and Smith R. M. (1977) *Critical Stability Constants*. Plenum Press, New York, NY.

Martinez R. E. and Ferris F. G. (2001) Chemical equilibrium modeling techniques for the analysis of high-resolution bacterial metal sorption data. *J. Colloid Interf. Sci.* **243**, 73–80.

Martinez R. E., Smith D. S., Kulczycki E. and Ferris F. G. (2002) Determination of intrinsic bacterial surface acidity constants using a Donnan shell model and a continuous pK_a distribution method. *J. Colloid Interf. Sci.* **253**, 130–139.

McCarthy J. F. and Zachara J. M. (1989) Subsurface transport of contaminants. *Environ. Sci. Technol.* **23**, 496–502.

Phoenix V. R., Adams D. G. and Konhauser K. O. (2000) Cyanobacterial viability during hydrothermal biomineralization. *Chem. Geol.* **169**, 329–338.

Phoenix V. R., Martinez R. E., Konhauser K. O. and Ferris F. G. (2002) Characterization and implications of the cell surface reactivity of the cyanobacteria *Calothrix* sp. *App. Environ. Microbiol.* **68**, 4827–4834.

Putney L. K., Denker S. P. and Barber D. L. (2002) The changing face of the Na^+/H^+ exchanger, NHE1: structure, regulation, and cellular actions. *Annu. Rev. Pharmacol. Toxicol.* **42**, 527–552.

Rippka R., Deruelles J., Waterbury J. B., Herdman M. and Stanier R. Y. (1979) Generic assignments, strain histories and properties of pure cultures of cyanobacteria. *J. Gen. Microbiol.* **111**, 1–61.

Smith D. S. and Kramer J. R. (1999) Multi-site proton interactions with natural organic matter. *Environ. Int.* **25**, 307–314.

Smith D. S., Adams N. W. H. and Kramer J. R. (1999) Resolving uncertainty in chemical speciation determinations. *Geochim. Cosmochim. Acta* **63**, 3337–3347.

van Loosdrecht M. C. M., Lyklema J., Norge W., Schraa G. and Zehnder A. J. B. (1987) Electrophoretic mobility and hydrophobicity as a measure to predict the initial steps of bacterial adhesion. *Appl. Environ. Microbiol.* **53**, 1898–1901.

van Loosdretch M. C. M., Lyklema J., Norde W. and Zehnder A. J. B. (1989) Bacterial adhesion: a physicochemical approach. *Microbial Ecol.* **17**, 1–15.

Waditee R., Hibino T., Tanaka Y., Nakamura T., Incharoensakdi A. and Takabe T. (2002) Overexpression of Na^+/H^+ antiporter confers the salt tolerance of freshwater cyanobacterium capable of growth in sea water. *Proc. Natl. Acad. Sci. USA* **99**, 4109–4114.

Walker S. L., Hill J. E., Redmon J. A. and Menachem E. (2005) Influence of growth phase on adhesion kinetics of *Escherichia coli* D21g. *Appl. Environ. Microbiol.* **71**, 3093–3099.

Warren L. A. and Ferris F. G. (1998) Continuum between sorption and precipitation of Fe(III) on microbial surfaces. *Environ. Sci. Technol.* **32**, 2331–2337.

Wrangstadh M., Conway P. L. and Kjelleberg S. (1986) The production of an extracellular polysaccharide during starvation of a marine *Pseudomonas* sp. and the effect thereof on adhesion. *Arch. Microbiol.* **14**, 220–227.

Yee N., Benning L. G., Pheonix V. R. and Ferris F. G. (2004) Characterization of metal-cyanobacteria sorption reactions: A combined macroscopic and infrared spectroscopic investigation. *Environ. Sci. Technol.* **38**, 775–782.

Zita A. and Hermansson M. (1997) Effects of bacterial cell surface structures and hydrophobicity on attachment to activated sludge flocs. *Appl. Environ. Microbiol.* **63**, 1168–1170.

Associate editor: Lesley A. Warren